(12)

AD-A184 835

High-Resolution Absorption Spectroscopy of NO_2

J. B. KOFFEND, J. S. HOLLOWAY, M. A. KWOK,
and R. F. HEIDNER III
Aerophysics Laboratory
Laboratory Operations
The Aerospace Corporation
El Segundo, CA 90245

31 August 1987

Prepared for

SPACE DIVISION
AIR FORCE SYSTEMS COMMAND
Los Angeles Air Force Station
P.O. Box 92960, Worldway Postal Center
Los Angeles, CA 90009-2960

This report was submitted by The Aerospace Corporation, El Segundo, CA 90245, under Contract No. F04701-85-C-0086-P00016 with the Space Division, P. O. Box 92960, Worldway Postal Center, Los Angeles, CA 90009-2960. It was reviewed and approved for The Aerospace Corporation by W. P. Thompson, Jr., Director, Aerophysics Laboratory.

Lt Scott W. Levinson/CNW was the project officer for the Mission-Oriented Investigation and Experimentation (MOIE) Program.

This report has been reviewed by the Public Affairs Office (PAS) and is releasable to the National Technical Information Service (NTIS). At NTIS, it will be available to the general public, including foreign nationals.

This technical report has been reviewed and is approved for publication. Publication of this report does not constitute Air Force approval of the report's findings or conclusions. It is published only for the exchange and stimulation of ideas.

Scott W. Levinson

SCOTT W. LEVINSON, Lt, USAF
MOIE Project Officer
SD/CNW

Joseph Hess

JOSEPH HESS, GM-15
Director, AFSTC West Coast Office
AFSTC/WCO OL-AB

UNCLASSIFIED
SECURITY CLASSIFICATION OF THIS PAGE

ADA184835

REPORT DOCUMENTATION PAGE

1a. REPORT SECURITY CLASSIFICATION Unclassified	1b. RESTRICTIVE MARKINGS
2a. SECURITY CLASSIFICATION AUTHORITY 2b. DECLASSIFICATION / DOWNGRADING SCHEDULE	3. DISTRIBUTION / AVAILABILITY OF REPORT Approved for public release; distribution unlimited
4. PERFORMING ORGANIZATION REPORT NUMBER(S) TR-0086A(2930-05)-1	5. MONITORING ORGANIZATION REPORT NUMBER(S) SD TR-87- 46
6a. NAME OF PERFORMING ORGANIZATION The Aerospace Corporation Laboratory Operations 6b. OFFICE SYMBOL (If applicable)	7a. NAME OF MONITORING ORGANIZATION Space Division
6c. ADDRESS (City, State, and ZIP Code) El Segundo, CA 90245	7b ADDRESS (City, State, and ZIP Code) Los Angeles Air Force Station Los Angeles, CA 90009-2960
8a. NAME OF FUNDING / SPONSORING ORGANIZATION 8b. OFFICE SYMBOL (If applicable)	9. PROCUREMENT INSTRUMENT IDENTIFICATION NUMBER F04701-85-C-0086-P00016
8c. ADDRESS (City, State, and ZIP Code)	10 SOURCE OF FUNDING NUMBERS PROGRAM ELEMENT NO. / PROJECT NO. / TASK NO. / WORK UNIT ACCESSION NO.

11 TITLE (Include Security Classification)
High-Resolution Absorption Spectroscopy of NO_2

12. PERSONAL AUTHOR(S) John B. Koffend, John S. Holloway, Munson A. Kwok, Raymond F. Heidner III

13a. TYPE OF REPORT	13b. TIME COVERED	14. DATE OF REPORT (Year, Month, Day)	15. PAGE COUNT
	FROM ____ TO ____	31 August 1987	31

16. SUPPLEMENTARY NOTATION

17. COSATI CODES			18 SUBJECT TERMS (Continue on reverse if necessary and identify by block number)
FIELD	GROUP	SUB-GROUP	Atmospheric propagation, Laser spectroscopy, Nitrogen dioxide, Spectroscopy

19. ABSTRACT (Continue on reverse if necessary and identify by block number)

The absorption cross section of NO_2 has been measured above the 3979-Å predissociation limit in the region of 3920 and 3950 Å, as well as in the discretely structured areas around 4112 and 4140 Å. Spectra were taken in a dual-beam arrangement by means of a tunable, pulsed dye laser having a 0.05-Å bandwidth (FWHM). This represents an improvement of at least a factor of three over the resolution employed in previous studies. Below 3979 Å, the spectra are continuous, with occasional diffuse rotational lines superimposed. The spectra taken above 4100 Å reveal a wealth of structural complexity. We report here absolute cross sections taken at 300 K. The work above 4100 Å was also performed at 250 K. Only slight variations in the measured cross sections are observed between these two temperatures.

20. DISTRIBUTION / AVAILABILITY OF ABSTRACT ☒ UNCLASSIFIED/UNLIMITED ☐ SAME AS RPT. ☐ DTIC USERS	21. ABSTRACT SECURITY CLASSIFICATION Unclassified
22a. NAME OF RESPONSIBLE INDIVIDUAL	22b. TELEPHONE (Include Area Code) / 22c. OFFICE SYMBOL

DD FORM 1473, 84 MAR — 83 APR edition may be used until exhausted. All other editions are obsolete.

SECURITY CLASSIFICATION OF THIS PAGE
Unclassified

CONTENTS

FIGURES

I. INTRODUCTION

Despite the great amount of effort that has been devoted to the study of the NO_2 absorption spectrum, a concise interpretation of the observed features has yet to be made. Actual state-to-state assignments in the visible and near UV have been possible only in certain instances.[1,2] This result is due in part to instrumental limitations, which are nonetheless continually being eliminated with the advent of narrow-bandwidth laser sources. The principal obstacle to a more complete understanding derives from the considerable complexity of the system under investigation, NO_2 being one of the classic examples of an ill-behaved small polyatomic molecule.[3] A detailed understanding of the spectroscopy of this region is of interest for a number of reasons. The photodissociation of NO_2 below 4200 Å and the increasing presence of NO_2 as an atmospheric pollutant combine to make this gas an important participant in the chemistry of the lower atmosphere. Current interest in the propagation of H_2 and D_2 Stokes-shifted xenon fluoride excimer-pumped wavelengths has reinforced the need for quantitative, high-resolution measurement of the NO_2 absorption cross section in the 3920 to 3950-Å and 4110 to 4150-Å regions of the spectrum.

Previous work in the 4000-Å region has revealed a complex and irregular structure. To the blue of 4000 Å, the spectrum is essentially continuous. On the basis of the onset of rotational diffuseness,[1] Douglas and Huber have placed the predissociation limit at 3979 Å. While partial assignments of bands to the $^2B_2 \leftarrow {}^2A_1$ and $^2B_1 \leftarrow {}^2A_1$ systems have been made in some cases, extensive electronic perturbation and vibronic coupling to the ground state have precluded a more complete delineation of the observed features.[4] Quantitative absorption measurements in the region have been hampered by relatively low spectral resolution. Left open to question has been the degree to which continuous absorption contributes to the spectrum as a whole. We report here the measurement of the absolute-absorption cross section of NO_2 from 3910 to 3925 Å, 3948 to 3953 Å, 4107 to 4115 Å, and 4131 to 4145 Å (air wavelength) taken at a bandwidth of 0.05 Å by means of a tunable, pulsed dye laser. All measurements were performed at 300 K and at several pressures of N_2 diluent ranging from 20 to 400 Torr. Measurements were also performed from 4107 to 4112.5 Å and 4132 to 4143 Å at 251 K.

II. EXPERIMENTAL PROCEDURE

Figure 1 depicts our experimental arrangement. The absorption measurements were carried out in a jacketed Pyrex cell of 5 cm diameter and 150 cm pathlength, equipped with wedged quartz thermopane windows. The cell was thermally insulated. For experiments at reduced temperature, we maintained a constant temperature (±0.5°C) over 95% of the pathlength, as determined prior to the experiment by means of an axially mounted thermocouple that could be positioned along the entire length of the cell. Absorption was measured in slowly flowing, dilute mixtures of NO_2. The NO_2 samples were obtained as a certified (0.51±0.02%) dilution in N_2 (Matheson) and a certified (2480±70 ppm) dilution in air from the National Bureau of Standards (SRM 2656). They were used without further purification. All samples were cross-calibrated against measurements performed on static samples of NO_2 purified by vacuum distillation. The high-pressure side of the gas-handling system was constructed of stainless steel, while the low-pressure flow section was made of Pyrex tubing. Flow rates were measured by digital mass flowmeters (Tylan). The cell pressure was determined by capacitance manometers (MKS) of 10 and 0.1 mTorr resolution. The cell temperature was monitored by thermocouples located at the midpoint and inner windows of the cell.

The output of an excimer-pumped dye laser (Lambda Physik) was collimated to a 5-mm diameter and directed into the absorption cell via uncoated Suprasil beam splitters. The beam was further attenuated by the use of smoked-glass, neutral-density filters of the appropriate optical density to avoid both saturation of the detectors and depletion of the NO_2 sample through photodissociation. The energy of the 15-nsec pulse was on the order of 10 nJ. Before the attenuated beam encountered the final turning flat, a portion of it was picked off by a wedged Suprasil beam splitter and directed to the reference detector. Matched Si photodiodes were used as detectors on the cell and reference legs of the apparatus. Wedged windows and beam splitters were employed in order to prevent low-level etalon effects. The undeviated portion of the main beam beyond the first turning flat was split off twice more, to

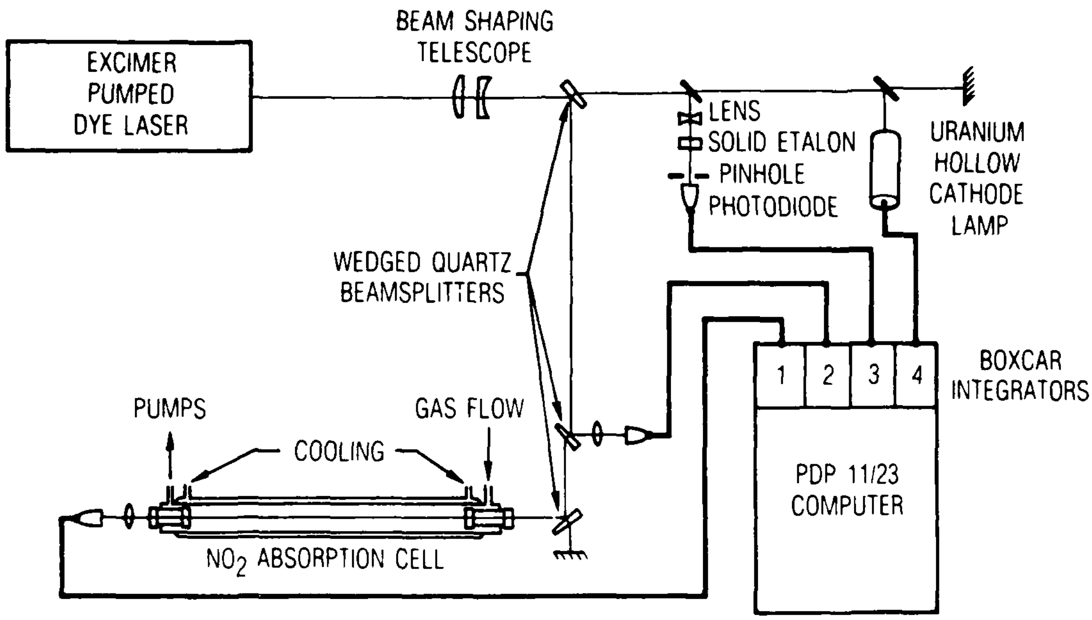

Fig. 1. Schematic Diagram of the Dual-Beam Absorption Apparatus. The four data channels employed for the measurements are indicated. Signals from the cell and reference photodiodes were balanced by adjustment of the position of the boxcar sampling gate on the exponentially decaying tail of the diode pulse.

the third and fourth channels of the experiment. One portion of the beam was expanded and then directed through a solid quartz etalon. The resulting fringes were scanned past a pinhole onto a photodiode, thus providing relative frequency calibration. A second portion of the beam was directed down the bore of a uranium (U) hollow cathode lamp. The coincidence of the scanning laser with a U atomic resonance produced a measurable ac fluctuation in the lamp voltage via the optogalvanic effect, thereby providing absolute wavelength calibration.[5] The four channels of the experiment were synchronously sampled by boxcar integrators (SRS) operating on a time constant consistent with our laser scan rate and pulse frequency (0.5 Å/min and 20 Hz, respectively). The boxcar outputs were digitized and stored on an LSI 11/23 lab computer (DEC).

The results of the comparison between our pure sample of NO_2 and the National Bureau of Standards (NBS) mixture were well within the stated limits of error, and allowed us to determine the concentration of the Matheson sample to be 0.49±0.01%. At room temperature the equilibrium partial pressure of N_2O_4 in the range of pressures used here was less than 0.1% that of NO_2, and could be effectively neglected in the determination of the absorption cross section. At 250 K, however, N_2O_4 is present in significant concentration (6.5% that of the NO_2 density). The absorption cross section of N_2O_4 is vanishingly small above 4000 Å.[6] It was therefore necessary to account for only the contribution of the equilibrium partial pressure of the dimer when calculating the cross section of NO_2 at reduced temperature.[6]

Attention was also paid to the flow rates employed, so as to assure that equilibrium was attained in the flowing sample prior to the sample's entrance into the absorption path. For our dilute samples, equilibrium between NO_2 and N_2O_4 in the low-pressure section of the apparatus was reached in all cases within 100 msec. At 400 Torr total pressure, plug-flow velocities were on the order of 80 cm/sec in the 60-cm-long gas inlet tubing, decreasing to about 3 cm/sec in the absorption cell. In the reduced-temperature portion of the experiment, equilibrium necessarily had to be reached after the sample entered the cooled cell. The inner thermopane entrance window extended 5 cm beyond the gas inlet, and in this instance also the sample was equilibrated prior to measurement. However, in the case of pure NO_2 at 100 mTorr, equilibration times were long enough to require the use of static samples.

A typical experiment consisted of a number of scans of 10 to 30 min in duration. Prior to and after the absorption measurements, background scans of the wavelength region were performed with an N_2 purge flowing through the cell at a rate equivalent to that of the NO_2 sample. These scans were consistently found to agree with one another to within 0.1% of full scale. The average of these scans constituted the baseline of our measurements. A flow of the NO_2 mixture would then be established and monitored at a fixed wavelength until a constant value was obtained. Spectra would subsequently be taken at several pressures over a given wavelength range. Partial pressures of NO_2 were on the order of 100 to 250 mTorr.

III. RESULTS AND DISCUSSION

The high-resolution, room-temperature spectrum of NO_2 in the 4110-Å region is presented in Figs. 2 and 3. Each plot represents the average of scans taken at two to three different partial pressures of NO_2, each scan being the result of a ratio of the signal from the cell detector to that of the reference detector normalized according to the baseline scans. We estimate our spectral accuracy to be ±0.02 Å. The error in the cross section is about ±5%, which results from uncertainties in the concentration of our NO_2 samples and the maximum variation between repetitive scans. Absorption cross sections have been measured in this region previously; however, because the resolution at which we have performed our measurements is from three to two hundred times greater than that of earlier work, comparison is ambiguous.[6,7] In the Appendix, the high-resolution computation of the absolute absorption coefficient is given for the 4100 to 4150-Å region. The NO_2 spectrum below 4100 Å has been studied exhaustively by Bass et al.,[8] and that work provides a direct comparison to the measurements performed at 3910 and 3948 to 3953 Å in this study. Figures 4 and 5 present our results in this region. The dashed lines connect the data points reported by Bass. The agreement in the cross-section is quite good, within 5 to 6%, our values being consistently lower than those reported by Bass. There is an apparent discrepancy in wavelength, amounting to an approximately 0.5-Å shift to the blue of Bass's data with respect to our own. A comparison of our wavelength calibration to the assignment of the band system at 3910 Å by Douglas and Huber shows excellent agreement (Fig. 6), and we believe this verifies our wavelength assignment.[1] Shifting Bass's data to the red by 0.5 Å results in an even closer agreement between the two data sets.

The effects of temperature and pressure were also explored in the region above 4100 Å. For a given partial pressure of NO_2, N_2 pressure was varied from 40 to 400 Torr. Within our limits of error, no observable change was evident in either the magnitude or the shape of the absorption features (Fig. 7). The absorption cell's temperature was also reduced to 252 K for a series

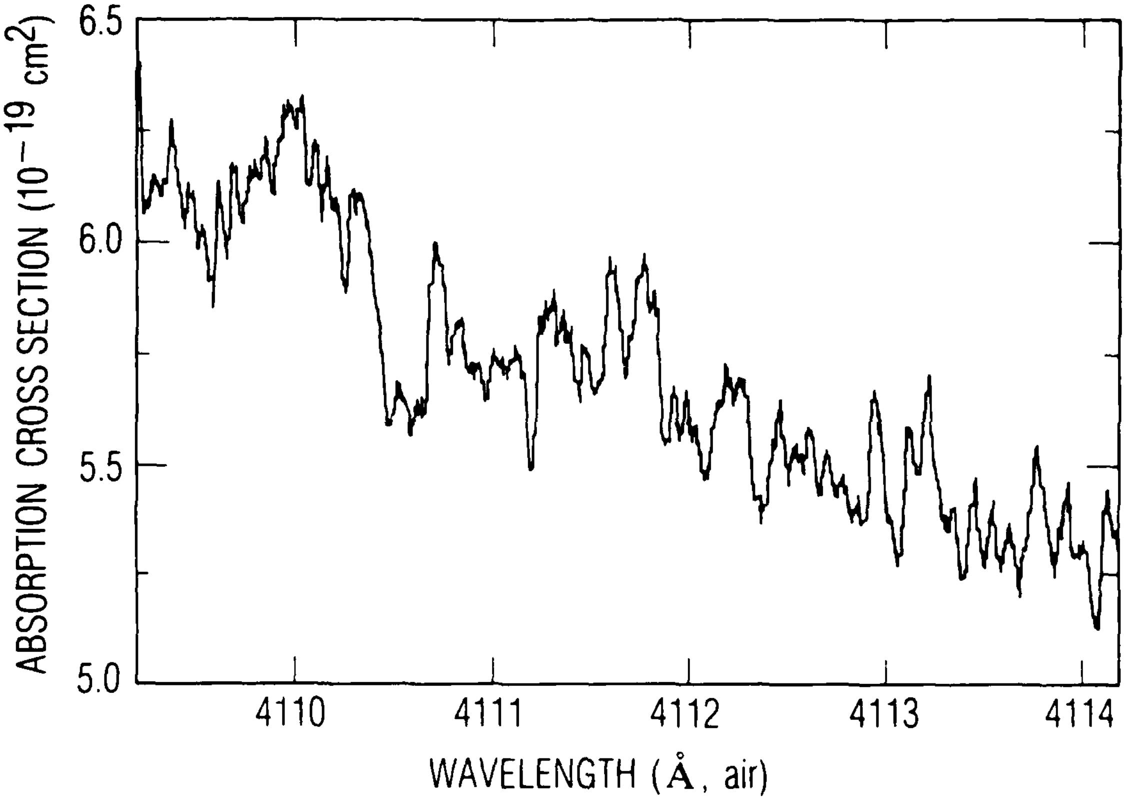

Fig. 2. Absolute Absorption Cross Section of NO_2 from 4109.2 to 4114.0 Å at T = 300 K.

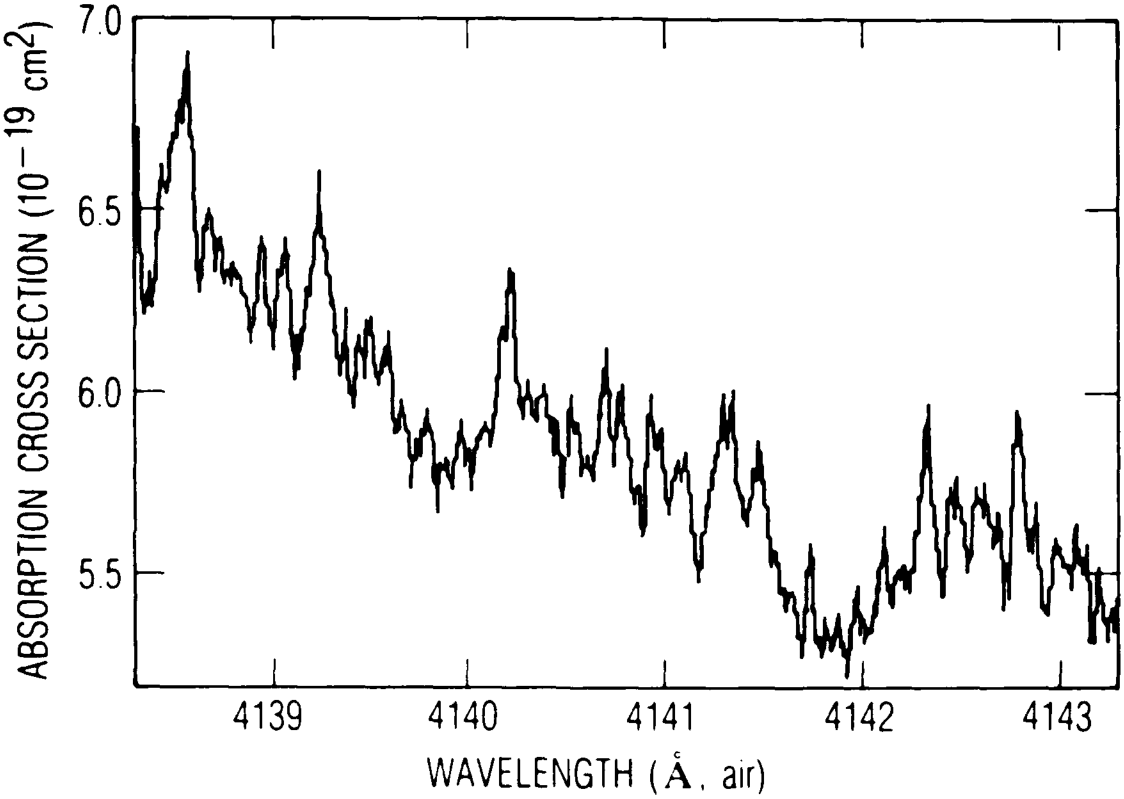

Fig. 3. Absolute Absorption Cross Section of NO_2 from 4138.3 to 4143.3 Å at T = 300 K.

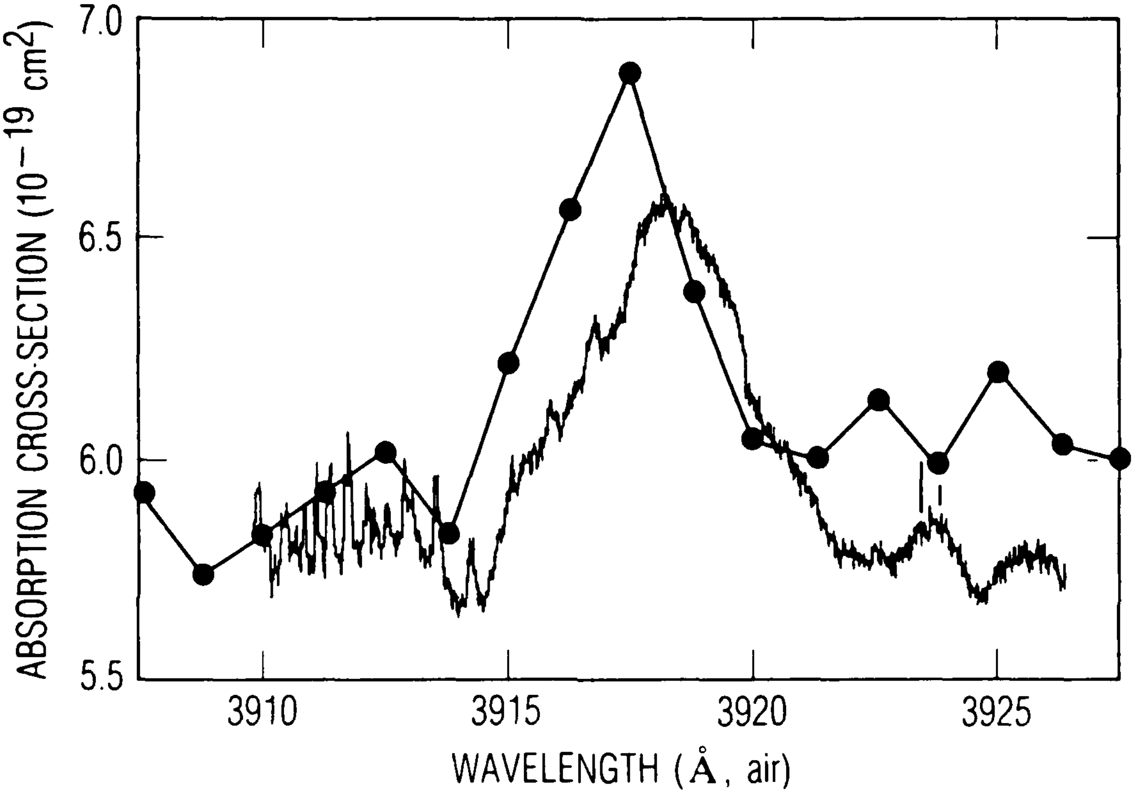

Fig. 4. Absolute Absorption Cross Section of NO_2 from 3910.0 to 3926.4 Å at T = 300 K. The dashed line connects data points reported by Bass et al.[8]

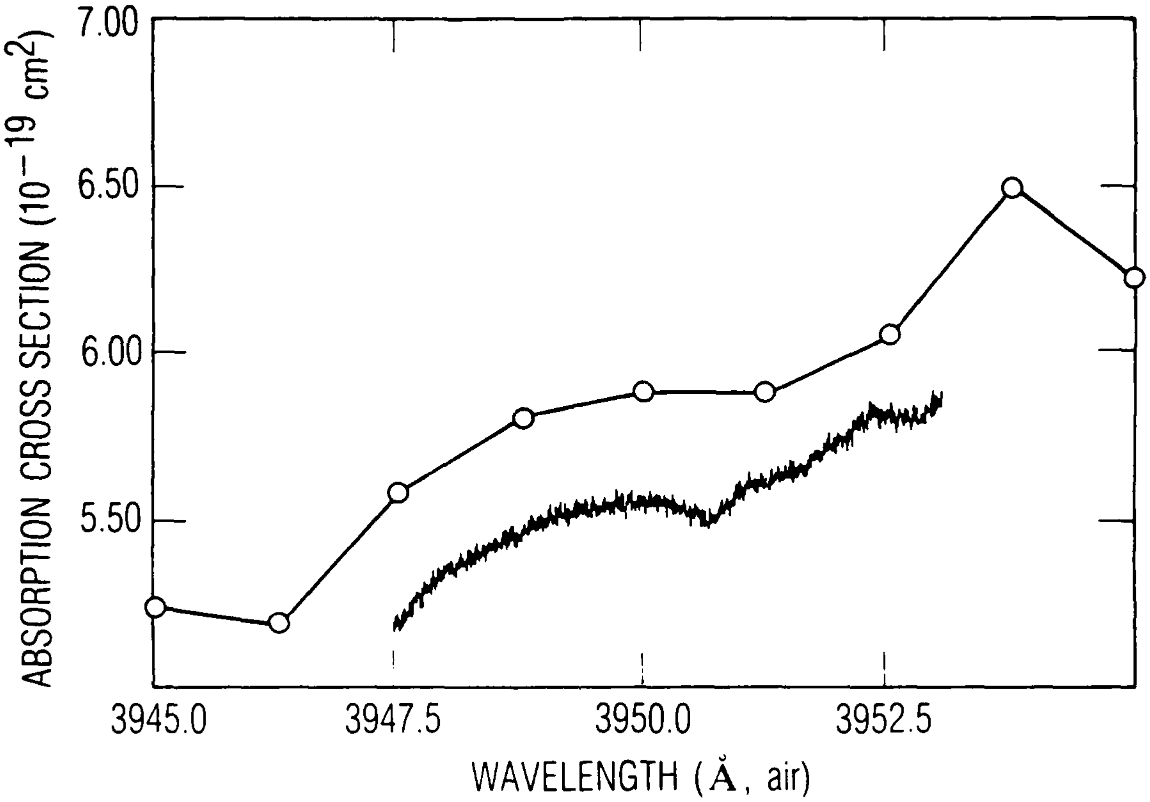

Fig. 5. Absolute Absorption Cross Section of NO_2 from 3948.0 to 3953.0 Å at T = 300 K. The dashed line connects data points reported by Bass et al.[8]

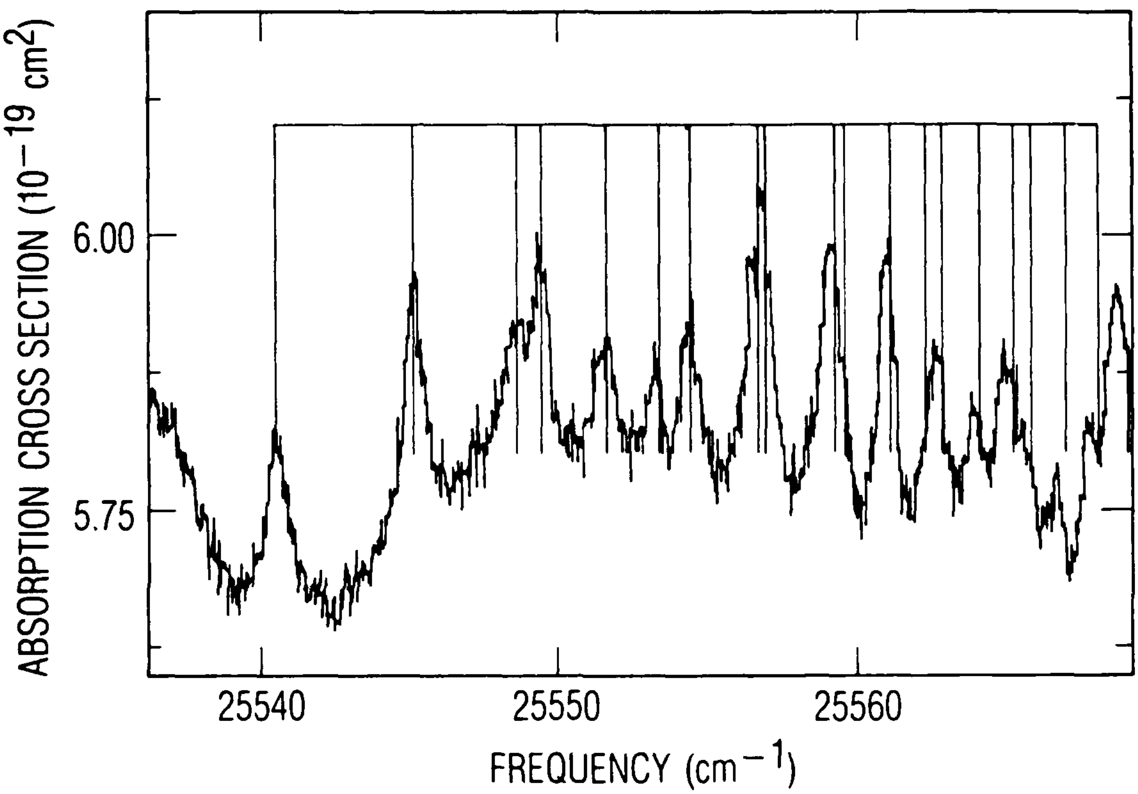

Fig. 6. The $^2B_1 \leftarrow {}^2A_1$ Band System of NO_2 at 3910 Å. The vertical lines denote the frequency assignments of Douglas and Huber.[1]

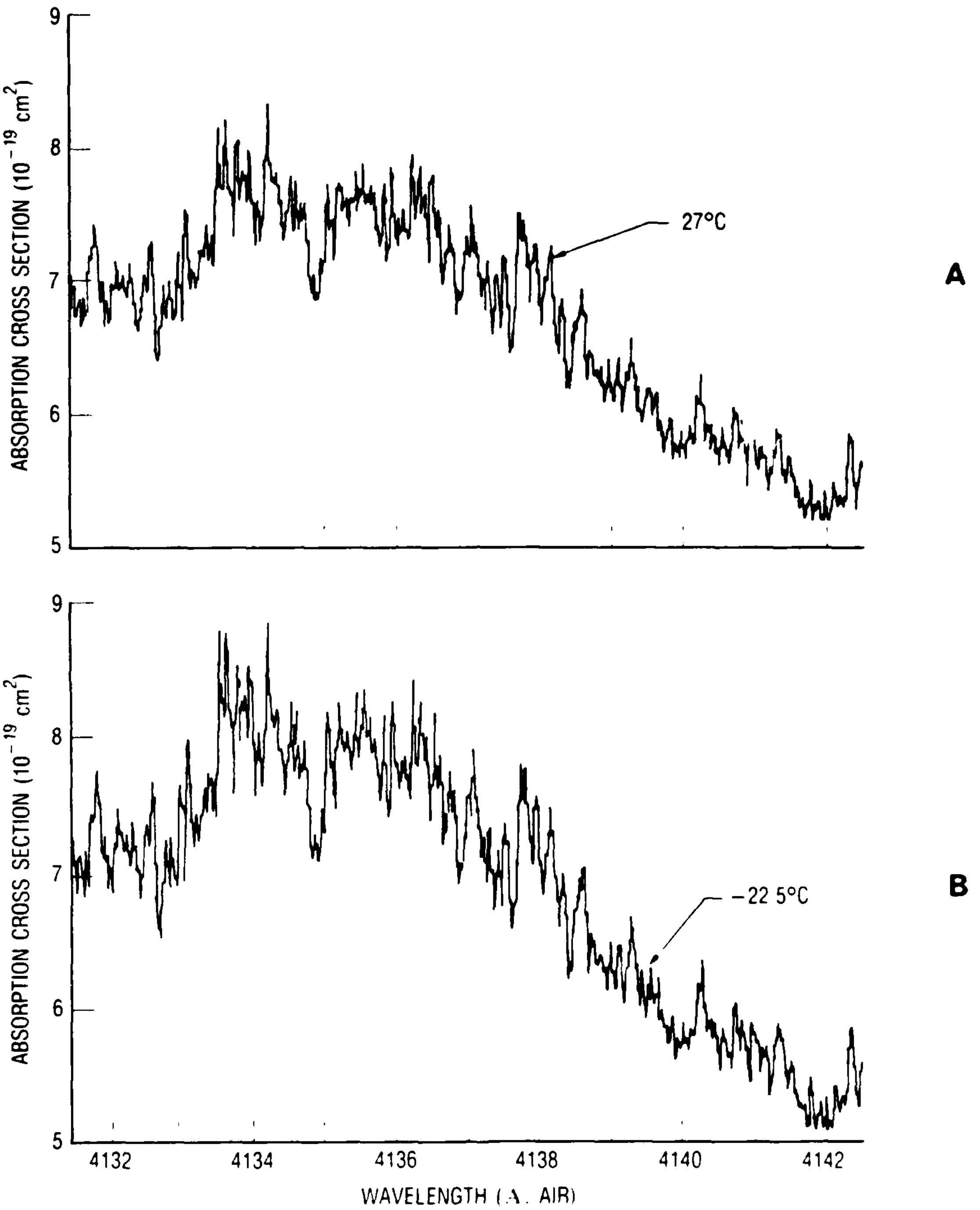

Fig. 7. Absorption Spectra of NO_2 at Room Temperature (a) and at 250.7 K (b). Note that the absorption cross section ordinate is magnified.

of measurements. Only slight changes in the magnitude of certain features were observed. A ratio of the cross sections of scans at 300 K to scans at 252 K varies from unity by no more than ±5%.

The predominance of continuum absorption below 398 nm has been well characterized and, in the predissociative regime, has been attributed by Rohlfing and Valentini to a crossing from the $^2B_2$ state to the $^2A_1$ ground state.[9] A qualitative understanding of the rather chaotic absorption spectrum in the 410 to 420-nm region, some 900 cm^{-1} below the predissociation threshold, may well require that many of the same arguments that have been presented for the 3900-Å region be invoked here. The NO quantum yield following excitation of NO_2 at 410 nm has been reported to be about 10%.[10] Uselman and Lee report the NO_2 fluorescence yield there to be greater than 90%.[11] In addition, the anomalously long radiative lifetime (t_{rad} = 74 μsec) suggests coupling to the dense quasi-continuum of the $^2A_1$ ground-state vibrational manifold.[3,12] The crossing presumably proceeds along the ν_3 asymmetric stretch coordinate of the $^2B_2$ state, which is also thought to be the dissociative channel for those species having requisite internal energy, while motion along the ν_1 symmetric stretch and the ν_2 bending coordinates acts as a reservoir for fluorescing species.[9,13] At longer wavelengths, radiative lifetimes have been shown to be strongly dependent on the excited state and in turn on the degree of mixing with the ground state. Lifetimes from 0.5 to 3.7 μsec have been reported for unperturbed levels of the $^2B_1$ state from 4544 to 4550 Å, a result that is in agreement with the value predicted by the integrated absorption coefficient, while transitions at 5934.5 Å attributed to the same electronic state display lifetimes of greater than 100 μsec as oscillator strength is spread among the perturbing levels.[14,15] A first step toward attaining a greater understanding of the region under current investigation, where predissociation is still thermally accessible, would entail making high-resolution measurements of both NO_2 photolysis and fluorescence yields, as well as time histories of the evolution of individual emission features. Work in this direction is presently under consideration in this laboratory.

IV. CONCLUSION

High-resolution absorption spectra of NO_2 have been obtained at 4112 and 4140 Å near the maximum of the NO_2 UV-visible absorption system. Spectra have also been taken at 3920 Å below the predissociation limit. The corresponding absorption cross sections are reported. The spectra above 4110 Å are densely and irregularly structured, while those below 3979 Å display an uninterrupted continuum containing the diffuse band system previously identified by Douglas and Huber.

REFERENCES

1. A. E. Douglas and K. P. Huber, Can. J. Phys. 43, 74 (1965).
2. R. E. Smalley, L. Wharton, and D. H. Levy, J. Chem. Phys. 63, (1975).
3. J. C. D. Brand and A. R. Hoy, J. Mol. Spec. 65, 55 (1977).
4. C. F. Jackels and E. R. Davidson, J. Chem. Phys. 65, 2941 (1976).
5. B. A. Palmer, R. A. Keller, and R. Engleman, Jr., "An Atlas of Uranium Emission Intensities in a Hollow Cathode Discharge," LA-8251-MS Informal Report, UC-34a, UC-LASL, Los Alamos, NM (July 1980).
6. T. C. Hall and F. E. Blacet, J. Chem. Phys. 20, 1745 (1952).
7. H. S. Johnston and R. Graham, Can. J. Chem. 52, 1415 (1973).
8. A. M. Bass, A. E. Ledford, and A. H. Laufer, J. Res. NBS 80A, 143 (1976).
9. E. A. Rohlfing and J. J. Valentini, J. Chem. Phys. 83, 521 (1985).
10. A. B. Harker, W. Ho, and J. J. Ratto, Chem. Phys. Lett. 50, 394 (1977).
11. W. M. Uselman and E. K. C. Lee, J. Chem. Phys. 64, 3457 (1976).
12. A. E. Douglas, J. Chem. Phys. 45, 1007 (1966).
13. J. N. Pitts, J. H. Sharp, and S. I. Chan, J. Chem. Phys. 42, 3655, (1964).
14. P. B. Sackett and J. T. Yardley, Chem. Phys. Lett. 9, 612 (1971).
15. C. G. Stevens, M. W. Swagle, R. Wallace, and R. N. Zare, Chem. Phys. Lett. 18, 465 (1973).

APPENDIX:

HIGH-RESOLUTION NO_2 ABSORPTION SPECTROSCOPY

R.F. Heidner, J.S. Holloway, M.A. Kwok, and J.B. Koffend
The Aerospace Corporation
Aerophysics Laboratory
Box 92957
Los Angeles, California 90009

The absorption spectrum of NO_2 near the H_2 Raman shifted XeF laser lines at 411 and 414 nm has been measured with a resolution of 0.006 nm with an excimer pumped dye laser. Wavelength calibration was performed using the opto-galvanic effect in a uranium hollow cathode lamp. The attached table lists the NO_2 absorption coefficients at room temperature in the wavelength regions near the shifted XeF lines. The estimated wavelength error is 0.001 nm. Spectra were also recorded at 251 K and the NO_2 absorption coefficients are identical to the room temperature values within our quoted experimental error of 5%.

NO_2 Absorption Cross Section (300K)

(Estimated error: wavelength +/- 0.001 nm; cross section +/- 5%)

Wavelength (nm)	Cross Section ($10^{-19}cm^2$)	Wavelength (nm)	Cross Section ($10^{-19}cm^2$)	Wavelength (nm)	Cross Section ($10^{-19}cm^2$)
410.920	6.38	411.090	5.72	411.260	5.58
410.921	6.40	411.091	5.71	411.261	5.57
410.922	6.32	411.092	5.70	411.262	5.54
410.923	6.20	411.093	5.73	411.263	5.48
410.924	6.10	411.094	5.71	411.264	5.44
410.925	6.08	411.095	5.68	411.265	5.44
410.926	6.08	411.096	5.67	411.266	5.47
410.927	6.09	411.097	5.65	411.267	5.51
410.928	6.12	411.098	5.66	411.268	5.49
410.929	6.14	411.099	5.69	411.269	5.50
410.930	6.12	411.100	5.73	411.270	5.49
410.931	6.12	411.101	5.74	411.271	5.46
410.932	6.12	411.102	5.74	411.272	5.45
410.933	6.12	411.103	5.73	411.273	5.42
410.934	6.12	411.104	5.73	411.274	5.42
410.935	6.15	411.105	5.73	411.275	5.44
410.936	6.19	411.106	5.74	411.276	5.46
410.937	6.27	411.107	5.71	411.277	5.46
410.938	6.25	411.108	5.71	411.278	5.45
410.939	6.23	411.109	5.72	411.279	5.42
410.940	6.18	411.110	5.72	411.280	5.40
410.941	6.14	411.111	5.71	411.281	5.37
410.942	6.11	411.112	5.73	411.282	5.38
410.943	6.09	411.113	5.76	411.283	5.42
410.944	6.06	411.114	5.75	411.284	5.42
410.945	6.07	411.115	5.73	411.285	5.38
410.946	6.09	411.116	5.71	411.286	5.36
410.947	6.12	411.117	5.68	411.287	5.36
410.948	6.10	411.118	5.62	411.288	5.40
410.949	6.08	411.119	5.56	411.289	5.48
410.950	6.02	411.120	5.51	411.290	5.56
410.951	5.99	411.121	5.49	411.291	5.63
410.952	6.01	411.122	5.54	411.292	5.66
410.953	6.02	411.123	5.66	411.293	5.64
410.954	5.99	411.124	5.76	411.294	5.62
410.955	5.96	411.125	5.81	411.295	5.58
410.956	5.92	411.126	5.82	411.296	5.56
410.957	5.90	411.127	5.84	411.297	5.50
410.958	5.87	411.128	5.85	411.298	5.46
410.959	5.95	411.129	5.84	411.299	5.40

NO_2 Absorption Cross Section (300K)

(Estimated error: wavelength +/- 0.001 nm; cross section +/- 5%)

Wavelength (nm)	Cross Section ($10^{-19}cm^2$)	Wavelength (nm)	Cross Section ($10^{-19}cm^2$)	Wavelength (nm)	Cross Section ($10^{-19}cm^2$)
410.960	6.06	411.130	5.86	411.300	5.39
410.961	6.12	411.131	5.87	411.301	5.37
410.962	6.12	411.132	5.84	411.302	5.36
410.963	6.06	411.133	5.79	411.303	5.33
410.964	6.00	411.134	5.78	411.304	5.33
410.965	5.99	411.135	5.80	411.305	5.29
410.966	6.00	411.136	5.83	411.306	5.31
410.967	6.02	411.137	5.83	411.307	5.36
410.968	6.09	411.138	5.80	411.308	5.43
410.969	6.15	411.139	5.77	411.309	5.54
410.970	6.18	411.140	5.80	411.310	5.57
410.971	6.17	411.141	5.80	411.311	5.58
410.972	6.10	411.142	5.75	411.312	5.57
410.973	6.06	411.143	5.69	411.313	5.53
410.974	6.06	411.144	5.68	411.314	5.49
410.975	6.07	411.145	5.68	411.315	5.48
410.976	6.09	411.146	5.71	411.316	5.49
410.977	6.12	411.147	5.75	411.317	5.52
410.978	6.14	411.148	5.76	411.318	5.58
410.979	6.14	411.149	5.74	411.319	5.65
410.980	6.15	411.150	5.72	411.320	5.68
410.981	6.16	411.151	5.68	411.321	5.68
410.982	6.16	411.152	5.66	411.322	5.60
410.983	6.16	411.153	5.67	411.323	5.50
410.984	6.15	411.154	5.67	411.324	5.48
410.985	6.22	411.155	5.69	411.325	5.46
410.986	6.18	411.156	5.69	411,326	5.44
410.987	6.14	411.157	5.71	411.327	5.40
410.988	6.12	411.158	5.72	411.328	5.38
410.989	6.13	411.159	5.79	411.329	5.35
410.990	6.17	411.160	5.86	411.330	5.36
410.991	6.17	411.161	5.93	411.331	5.36
410.992	6.20	411.162	5.93	411.332	5.39
410.993	6.23	411.163	5.94	411.333	5.39
410.994	6.28	411.164	5.89	411.334	5.40
410.995	6.28	411.165	5.88	411.335	5.32
410.996	6.28	411.166	5.83	411.336	5.26
410.997	6.30	411.167	5.76	411.337	5.24
410.998	6.30	411.168	5.71	411.338	5.25
410.999	6.30	411.169	5.72	411.339	5.28

NO_2 Absorption Cross Section (300K)

(Estimated error: wavelength +/- 0.001 nm; cross section +/- 5%)

Wavelength (nm)	Cross Section ($10^{-19}cm^2$)	Wavelength (nm)	Cross Section ($10^{-19}cm^2$)	Wavelength (nm)	Cross Section ($10^{-19}cm^2$)
411.000	6.27	411.170	5.78	411.340	5.33
411.001	6.26	411.171	5.80	411.341	5.37
411.002	6.29	411.172	5.85	411.342	5.41
411.003	6.29	411.173	5.91	411.343	5.45
411.004	6.31	411.174	5.92	411.344	5.46
411.005	6.27	411.175	5.92	411.345	5.45
411.006	6.21	411.176	5.95	411.346	5.39
411.007	6.13	411.177	5.97	411.347	5.32
411.008	6.13	411.178	5.94	411.348	5.30
411.009	6.16	411.179	5.90	411.349	5.26
411.010	6.19	411.180	5.84	411.350	5.29
411.011	6.22	411.181	5.85	411.351	5.31
411.012	6.18	411.182	5.86	411.352	5.37
411.013	6.11	411.183	5.89	411.353	5.38
411.014	6.06	411.184	5.83	411.354	5.37
411.015	6.07	411.185	5.79	411.355	5.35
411.016	6.12	411.186	5.68	411.356	5.30
411.017	6.17	411.187	5.59	411.357	5.27
411.018	6.18	411.188	5.55	411.358	5.28
411.019	6.12	411.189	5.56	411.359	5.30
411.020	6.09	411.190	5.55	411.360	5.30
411.021	6.07	411.191	5.60	411.361	5.33
411.022	6.07	411.192	5.65	411.362	5.35
411.023	6.07	411.193	5.66	411.363	5.32
411.024	6.01	411.194	5.63	411.364	5.29
411.025	5.95	411.195	5.58	411.365	5.24
411.026	5.91	411.196	5.55	411.366	5.21
411.027	5.93	411.197	5.57	411.367	5.25
411.028	6.05	411.198	5.64	411.368	5.30
411.029	6.09	411.199	5.66	411.369	5.31
411.030	6.10	411.200	5.60	411.370	5.31
411.031	6.08	411.201	5.57	411.371	5.31
411.032	6.10	411.202	5.58	411.372	5.37
411.033	6.09	411.203	5.57	411.373	5.42
411.034	6.10	411.204	5.56	411.374	5.45
411.035	6.07	411.205	5.56	411.375	5.51
411.036	6.03	411.206	5.54	411.376	5.53
411.037	6.04	411.207	5.50	411.377	5.51
411.038	6.02	411.208	5.47	411.378	5.45
411.039	5.96	411.209	5.48	411.379	5.42

NO_2 Absorption Cross Section (300K)

(Estimated error: wavelength +/- 0.001 nm; cross-section +/- 5%)

Wavelength (nm)	Cross Section ($10^{-19}cm^2$)	Wavelength (nm)	Cross Section ($10^{-19}cm^2$)	Wavelength (nm)	Cross Section ($10^{-19}cm^2$)
411.040	5.90	411.210	5.48	411.380	5.39
411.041	5.86	411.211	5.52	411.381	5.38
411.042	5.85	411.212	5.56	411.382	5.36
411.043	5.82	411.213	5.60	411.383	5.35
411.044	5.77	411.214	5.63	411.384	5.27
411.045	5.70	411.215	5.64	411.385	5.25
411.046	5.66	411.216	5.64	411.386	5.28
411.047	5.61	411.217	5.64	411.387	5.31
411.048	5.60	411.218	5.68	411.388	5.35
411.049	5.60	411.219	5.70	411.389	5.38
411.050	5.62	411.220	5.71	411.390	5.41
411.051	5.64	411.221	5.69	411.391	5.44
411.052	5.64	411.222	5.67	411.392	5.38
411.053	5.66	411.223	5.65	411.393	5.31
411.054	5.65	411.224	5.68	411.394	5.29
411.055	5.65	411.225	5.67	411.395	5.29
411.056	5.64	411.226	5.68	411.396	5.28
411.057	5.63	411.227	5.67	411.397	5.32
411.058	5.61	411.228	5.67	411.398	5.29
411.059	5.57	411.229	5.68	411.399	5.31
411.060	5.59	411.230	5.63	411.400	5.30
411.061	5.60	411.231	5.59	411.401	5.29
411.062	5.63	411.232	5.51	411.402	5.26
411.063	5.62	411.233	5.46	411.403	5.21
411.064	5.63	411.234	5.43	411.404	5.17
411.065	5.61	411.235	5.42	411.405	5.14
411.066	5.62	411.236	5.36	411.406	5.16
411.067	5.64	411.237	5.39	411.407	5.18
411.068	5.69	411.238	5.43	411.408	5.25
411.069	5.78	411.239	5.50	411.409	5.31
411.070	5.83	411.240	5.50	411.410	5.39
411.071	5.91	411.241	5.53	411.411	5.44
411.072	5.96	411.242	5.55	411.412	5.40
411.073	5.98	411.243	5.59	411.413	5.38
411.074	5.96	411.244	5.63	411.414	5.35
411.075	5.95	411.245	5.61	411.415	5.33
411.076	5.93	411.246	5.58	411.416	5.33
411.077	5.87	411.247	5.51	411.417	5.34
411.078	5.80	411.248	5.48	411.418	5.34
411.079	5.75	411.249	5.47	411.419	5.35

NO_2 Absorption Cross Section (300K)

(Estimated error: wavelength +/- 0.001 nm; cross section +/- 5%)

Wavelength (nm)	Cross Section ($10^{-19}cm^2$)	Wavelength (nm)	Cross Section ($10^{-19}cm^2$)
411.080	5.75	411.250	5.48
411.081	5.78	411.251	5.52
411.082	5.82	411.252	5.53
411.083	5.81	411.253	5.51
411.084	5.81	411.254	5.54
411.085	5.81	411.255	5.52
411.086	5.76	411.256	5.51
411.087	5.75	411.257	5.48
411.088	5.73	411.258	5.51
411.089	5.72	411.259	5.56

NO$_2$ Absorption Cross Section (300K)

(Estimated error: wavelength +/- 0.001 nm; cross section +/- 5%)

Wavelength (nm)	Cross Section ($10^{-19}cm^2$)	Wavelength (nm)	Cross Section ($10^{-19}cm^2$)	Wavelength (nm)	Cross Section ($10^{-19}cm^2$)
413.830	6.72	414.000	5.82	414.170	5.40
413.831	6.59	414.001	5.76	414.171	5.50
413.832	6.43	414.002	5.79	414.172	5.60
413.833	6.29	414.003	5.86	414.173	5.58
413.834	6.23	414.004	5.84	414.174	5.54
413.835	6.25	414.005	5.88	414.175	5.42
413.836	6.25	414.006	5.90	414.176	5.35
413.837	6.32	414.007	5.88	414.177	5.31
413.838	6.29	414.008	5.90	414.178	5.27
413.839	6.23	414.009	5.87	414.179	5.30
413.840	6.33	414.010	5.87	414.180	5.37
413.841	6.49	414.011	5.90	414.181	5.35
413.842	6.58	414.012	5.92	414.182	5.34
413.843	6.56	414.013	5.96	414.183	5.32
413.844	6.56	414.014	6.03	414.184	5.32
413.845	6.55	414.015	6.07	414.185	5.34
413.846	6.59	414.016	6.17	414.186	5.39
413.847	6.65	414.017	6.19	414.187	5.38
413.848	6.67	414.018	6.19	414.188	5.36
413.849	6.68	414.019	6.17	414.189	5.34
413.850	6.71	414.020	6.22	414.190	5.27
413.851	6.78	414.021	6.30	414.191	5.27
413.852	6.78	414.022	6.31	414.192	5.25
413.853	6.73	414.023	6.29	414.193	5.31
413.854	6.75	414.024	6.16	414.194	5.36
413.855	6.83	414.025	6.04	414.195	5.42
413.856	6.91	414.026	5.97	414.196	5.47
413.857	6.86	414.027	5.97	414.197	5.43
413.858	6.74	414.028	6.02	414.198	5.41
413.859	6.60	414.029	6.02	414.199	5.38
413.860	6.47	414.030	6.00	414.200	5.38
413.861	6.41	414.031	5.97	414.201	5.35
413.862	6.33	414.032	5.93	414.202	5.36
413.863	6.29	414.033	5.93	414.203	5.36
413.864	6.35	414.034	5.93	414.204	5.37
413.865	6.46	414.035	6.00	414.205	5.40
413.866	6.44	414.036	6.02	414.206	5.42
413.867	6.48	414.037	6.00	414.207	5.46
413.868	6.41	414.038	5.97	414.208	5.51
413.869	6.35	414.039	5.96	414.209	5.59

NO_2 Absorption Cross Section (300K)

(Estimated error: wavelength +/- 0.001 nm; cross section +/- 5%)

Wavelength (nm)	Cross Section ($10^{-19}cm^2$)	Wavelength (nm)	Cross Section ($10^{-19}cm^2$)	Wavelength (nm)	Cross Section ($10^{-19}cm^2$)
413.870	6.37	414.040	5.91	414.210	5.61
413.871	6.42	414.041	5.86	414.211	5.54
413.872	6.42	414.042	5.89	414.212	5.46
413.873	6.33	414.043	5.93	414.213	5.42
413.874	6.30	414.044	5.94	414.214	5.48
413.875	6.31	414.045	5.85	414.215	5.50
413.876	6.32	414.046	5.77	414.216	5.51
413.877	6.31	414.047	5.72	414.217	5.52
413.878	6.28	414.048	5.78	414.218	5.52
413.879	6.29	414.049	5.89	414.219	5.49
413.880	6.31	414.050	5.98	414.220	5.49
413.881	6.30	414.051	5.95	414.221	5.47
413.882	6.29	414.052	5.95	414.222	5.47
413.883	6.32	414.053	5.92	414.223	5.48
413.884	6.31	414.054	5.90	414.224	5.52
413.885	6.25	414.055	5.86	414.225	5.55
413.886	6.25	414.056	5.80	414.226	5.65
413.887	6.17	414.057	5.79	414.227	5.72
413.888	6.16	414.058	5.80	414.228	5.77
413.889	6.17	414.059	5.81	414.229	5.80
413.890	6.20	414.060	5.79	414.230	5.84
413.891	6.26	414.061	5.79	414.231	5.95
413.892	6.32	414.062	5.78	414.232	5.98
413.893	6.42	414.063	5.79	414.233	5.89
413.894	6.41	414.064	5.86	414.234	5.82
413.895	6.28	414.065	5.89	414.235	5.71
413.896	6.26	414.066	5.92	414.236	5.67
413.897	6.24	414.067	5.98	414.237	5.62
413.898	6.18	414.068	6.06	414.238	5.52
413.899	6.16	414.069	6.09	414.239	5.48
413.900	6.14	414.070	6.06	414.240	5.46
413.901	6.15	414.071	5.94	414.241	5.52
413.902	6.24	414.072	5.83	414.242	5.60
413.903	6.26	414.073	5.86	414.243	5.70
413.904	6.31	414.074	5.90	414.244	5.73
413.905	6.37	414.075	5.98	414.245	5.73
413.906	6.40	414.076	6.00	414.246	5.71
413.907	6.38	414.077	6.00	414.247	5.77
413.908	6.28	414.078	5.91	414.248	5.75
413.909	6.14	414.079	5.89	414.249	5.71

NO$_2$ Absorption Cross Section (300K)

(Estimated error: wavelength +/- 0.001 nm; cross section +/- 5%)

Wavelength (nm)	Cross Section ($10^{-19}cm^2$)	Wavelength (nm)	Cross Section ($10^{-19}cm^2$)	Wavelength (nm)	Cross-Section ($10^{-19}cm^2$)
413.910	6.10	414.080	5.86	414.250	5.66
413.911	6.04	414.081	5.76	414.251	5.62
413.912	6.11	414.082	5.73	414.252	5.56
413.913	6.10	414.083	5.71	414.253	5.60
413.914	6.14	414.084	5.75	414.254	5.74
413.915	6.16	414.085	5.75	414.255	5.72
413.916	6.19	414.086	5.66	414.256	5.73
413.917	6.26	414.087	5.57	414.257	5.72
413.918	6.30	414.088	5.58	414.258	5.71
413.919	6.32	414.089	5.71	414.259	5.71
413.920	6.35	414.090	5.89	414.260	5.69
413.921	6.42	414.091	5.97	414.261	5.77
413.922	6.57	414.092	5.96	414.262	5.72
413.923	6.56	414.093	5.92	414.263	5.66
413.924	6.56	414.094	5.87	414.264	5.63
413.925	6.44	414.095	5.87	414.265	5.62
413.926	6.42	414.096	5.89	414.266	5.62
413.927	6.38	414.097	5.90	414.267	5.62
413.928	6.29	414.098	5.89	414.268	5.67
413.929	6.28	414.099	5.80	414.269	5.66
413.930	6.25	414.100	5.74	414.270	5.60
413.931	6.19	414.101	5.68	414.271	5.46
413.932	6.12	414.102	5.71	414.272	5.45
413.933	6.05	414.103	5.74	414.273	5.48
413.934	6.04	414.104	5.79	414.274	5.57
413.935	6.09	414.105	5.82	414.275	5.72
413.936	6.21	414.106	5.81	414.276	5.87
413.937	6.21	414.107	5.79	414.277	5.96
413.938	6.11	414.108	5.81	414.278	5.90
413.939	5.99	414.109	5.79	414.279	5.92
413.940	5.99	414.110	5.79	414.280	5.90
413.941	5.97	414.111	5.74	414.281	5.83
413.942	6.02	414.112	5.74	414.282	5.71
413.943	6.11	414.113	5.60	414.283	5.64
413.944	6.13	414.114	5.54	414.284	5.58
413.945	6.11	414.115	5.52	414.285	5.60
413.946	6.04	414.116	5.49	414.286	5.62
413.947	6.12	414.117	5.57	414.287	5.67
413.948	6.20	414.118	5.65	414.288	5.69
413.949	6.19	414.119	5.70	414.289	5.64

NO_2 Absorption Cross Section (300K)

(Estimated error: wavelength +/- 0.001 nm; cross section +/- 5%)

Wavelength (nm)	Cross Section ($10^{-19}cm^2$)	Wavelength (nm)	Cross Section ($10^{-19}cm^2$)	Wavelength (nm)	Cross Section ($10^{-19}cm^2$)
413.950	6.19	414.120	5.65	414.290	5.53
413.951	6.17	414.121	5.72	414.291	5.45
413.952	6.13	414.122	5.78	414.292	5.40
413.953	6.02	414.123	5.81	414.293	5.41
413.954	6.01	414.124	5.81	414.294	5.46
413.955	6.05	414.125	5.82	414.295	5.56
413.956	6.07	414.126	5.93	414.296	5.58
413.957	6.07	414.127	5.99	414.297	5.60
413.958	6.12	414.128	5.98	414.298	5.57
413.959	6.14	414.129	5.93	414.299	5.57
413.960	6.04	414.130	5.92	414.300	5.57
413.961	5.92	414.131	5.95	414.301	5.57
413.962	5.90	414.132	6.01	414.302	5.55
413.963	5.90	414.133	5.98	414.303	5.52
413.964	5.97	414.134	5.89	414.304	5.49
413.965	5.99	414.135	5.77	414.305	5.47
413.966	5.94	414.136	5.69	414.306	5.50
413.967	5.89	414.137	5.69	414.307	5.59
413.968	5.81	414.138	5.71	414.308	5.64
413.969	5.78	414.139	5.68	414.309	5.60
413.970	5.78	414.140	5.67	414.310	5.54
413.971	5.82	414.141	5.69	414.311	5.52
413.972	5.88	414.142	5.71	414.312	5.55
413.973	5.84	414.143	5.72	414.313	5.59
413.974	5.85	414.144	5.76	414.314	5.57
413.975	5.83	414.145	5.79	414.315	5.49
413.976	5.90	414.146	5.85	414.316	5.36
413.977	5.93	414.147	5.85	414.317	5.32
413.978	5.97	414.148	5.80	414.318	5.40
413.979	5.96	414.149	5.75	414.319	5.48
413.980	5.90	414.150	5.71	414.320	5.50
413.981	5.85	414.151	5.66	414.321	5.47
413.982	5.79	414.152	5.57	414.322	5.40
413.983	5.68	414.153	5.53	414.323	5.37
413.984	5.75	414.154	5.55	414.324	5.33
413.985	5.81	414.155	5.54	414.325	5.35
413.986	5.82	414.156	5.53	414.326	5.36
413.987	5.83	414.157	5.46	414.327	5.38
413.988	5.81	414.158	5.44	414.328	5.40
413.989	5.77	414.159	5.42	414.329	5.43

NO$_2$ Absorption Cross Section (300K)

(Estimated error: wavelength +/- 0.001 nm; cross section +/- 5%)

Wavelength (nm)	Cross Section ($10^{-19}cm^2$)	Wavelength (nm)	Cross Section ($10^{-19}cm^2$)
413.990	5.74	414.160	5.43
413.991	5.79	414.161	5.44
413.992	5.84	414.162	5.43
413.993	5.87	414.163	5.45
413.994	5.90	414.164	5.43
413.995	5.92	414.165	5.45
413.996	5.87	414.166	5.36
413.997	5.82	414.167	5.33
413.998	5.83	414.168	5.31
413.999	5.83	414.169	5.33

LABORATORY OPERATIONS

The Aerospace Corporation functions as an "architect-engineer" for national security projects, specializing in advanced military space systems. Providing research support, the corporation's Laboratory Operations conducts experimental and theoretical investigations that focus on the application of scientific and technical advances to such systems. Vital to the success of these investigations is the technical staff's wide-ranging expertise and its ability to stay current with new developments. This expertise is enhanced by a research program aimed at dealing with the many problems associated with rapidly evolving space systems. Contributing their capabilities to the research effort are these individual laboratories:

Aerophysics Laboratory: Launch vehicle and reentry fluid mechanics, heat transfer and flight dynamics; chemical and electric propulsion, propellant chemistry, chemical dynamics, environmental chemistry, trace detection; spacecraft structural mechanics, contamination, thermal and structural control; high temperature thermomechanics, gas kinetics and radiation; cw and pulsed chemical and excimer laser development including chemical kinetics, spectroscopy, optical resonators, beam control, atmospheric propagation, laser effects and countermeasures.

Chemistry and Physics Laboratory: Atmospheric chemical reactions, atmospheric optics, light scattering, state-specific chemical reactions and radiative signatures of missile plumes, sensor out-of-field-of-view rejection, applied laser spectroscopy, laser chemistry, laser optoelectronics, solar cell physics, battery electrochemistry, space vacuum and radiation effects on materials, lubrication and surface phenomena, thermionic emission, photo-sensitive materials and detectors, atomic frequency standards, and environmental chemistry.

Computer Science Laboratory: Program verification, program translation, performance-sensitive system design, distributed architectures for spaceborne computers, fault-tolerant computer systems, artificial intelligence, micro-electronics applications, communication protocols, and computer security.

Electronics Research Laboratory: Microelectronics, solid-state device physics, compound semiconductors, radiation hardening; electro-optics, quantum electronics, solid-state lasers, optical propagation and communications; microwave semiconductor devices, microwave/millimeter wave measurements, diagnostics and radiometry, microwave/millimeter wave thermionic devices; atomic time and frequency standards; antennas, rf systems, electromagnetic propagation phenomena, space communication systems.

Materials Sciences Laboratory: Development of new materials: metals, alloys, ceramics, polymers and their composites, and new forms of carbon; non-destructive evaluation, component failure analysis and reliability; fracture mechanics and stress corrosion; analysis and evaluation of materials at cryogenic and elevated temperatures as well as in space and enemy-induced environments.

Space Sciences Laboratory: Magnetospheric, auroral and cosmic ray physics, wave-particle interactions, magnetospheric plasma waves; atmospheric and ionospheric physics, density and composition of the upper atmosphere, remote sensing using atmospheric radiation; solar physics, infrared astronomy, infrared signature analysis; effects of solar activity, magnetic storms and nuclear explosions on the earth's atmosphere, ionosphere and magnetosphere; effects of electromagnetic and particulate radiations on space systems; space instrumentation.